

# Simulation of arbitrarily complex 3-D layouts of SI POF. Losses in some non-planar bends of practical interest.

F. Jiménez <sup>1</sup>, J. Arrue <sup>1</sup>, M.A. Losada <sup>2</sup>, and J. Zubia <sup>1</sup>

<sup>1</sup> University of the Basque Country, Alda. Urquijo s/n, E-48013 Bilbao, Spain

<sup>2</sup> University of Zaragoza, María de Luna 3, E-50015 Zaragoza, Spain

E-mails: mapjihf@bi.ehu.es, jtpararj@bi.ehu.es

**Abstract.** Practical uses of step-index plastic optical fibres often involve layouts with complex three-dimensional bends, especially in short-distance applications with small spaces available (automotive industry, robotics, etc.). Therefore, the simulation of optical links with arbitrary non-planar geometries becomes of great interest. This paper employs a new computer program capable of simulating light propagation in such configurations to draw some conclusions in situations of practical interest.

## 1 Introduction

Many practical uses of step-index plastic optical fibres (SI POFs) involve layouts in which complex three-dimensional bends are needed (e.g. automotive industry, robotics, some LANs and sensors, etc.) [1]. Although quite precise computational simulations of light propagation in straight and circular POF sections have already been carried out [2,3], planar bends often have a variable curvature (e.g. in the form of a sine, or even shapes that cannot be expressed with an analytical expression), and many bends are not even planar, i.e., their fibre symmetry axes have a torsion. This tends to add some difficulty to the problem. The automotive industry, with its optical network through POF called MOST, provides many examples of this kind of 3-D optical link configurations for which no computational simulation tool developed until now is flexible enough. Therefore, we have developed a computer program based on the ray-tracing method that is able to simulate arbitrarily complex non-planar layouts, with two aims: firstly, to predict the behaviour (bend losses, bandwidth, etc.) of specific links with a given geometry at the design stage; and secondly, to try to draw rule-of-thumb conclusions that may be valid in a wider variety of situations, i.e., at an even earlier stage of design, when link geometry is not yet fully determined. In this paper we focus on bend losses in 3-D situations of practical interest, including the possibility of having perturbations in the ideally circular cross-section geometry along the POF axis.

As a first simple example, we carry out computational simulations to compare power losses in POFs bent in the shape of helices with those obtained along planar circular arcs, maintaining the local radius of curvature and the distance covered, to check to what extent the torsion present in a helix affects the results. A second analysis is that of the combined effect of two consecutive bends depending only on their relative positions in space, while keeping their respective radii and arc length constant. In the third place, we simulate attenuation incurred in practical installations in which bends of different radii can be found along the optical link, showing and explaining that the position of emitter and receiver usually cannot be interchanged without modifying bending losses. Finally, the field of sensing devices also provides many cases in which the ability to simulate arbitrary geometries can be of great value. For instance, a pressure sensor

based on the deformation of the fibre [4] can be easily simulated by the program, as will be done to illustrate its capabilities.

## 2 Modelling three-dimensionally bent POFs with variable cross-section

We will now describe the implementation of the simulation program very briefly. It allows to apply the ray-tracing method to the simulation of light propagation in SI POFs of very flexible geometry –namely, of fibre axes following practically any 3D trajectory and of cross sections whose size, shape and orientation are also allowed to vary in a very general way. This can be applied to any reasonable fibre geometry that could be found in practice.

For the sake of flexibility, it is very convenient to define the fibre geometry as a separate software module (typically a “function” written in a programming language). The propagation of light rays is calculated in another, independent function. The former returns the centre  $c$  of the fibre symmetry axis, its tangent  $t$ , the cross section main axes  $x$  and  $y$ , the half-axes  $a$  and  $b$ , and the degree of homogeneity  $m$ , as a function of a certain parameter  $p$ , which could be the distance along the fibre axis or any other one. If  $m = 2$ , the cross-section is an ellipse; if, additionally,  $a = b$ , it is a circle, according to:

$$\left(\frac{x}{a}\right)^m + \left(\frac{y}{b}\right)^m = 1 \quad (1)$$

as proposed by [5].

Cross-sections with different equations than (1) are almost as easy to implement, but we will use this one. To calculate the ray reflection points, the following slack function can be defined and calculated in a straightforward manner for any value of  $p$ :

$$S(p) = 1 - \left(\frac{x(p)}{a(p)}\right)^{m(p)} - \left(\frac{y(p)}{b(p)}\right)^{m(p)} \quad (2)$$

where  $x(p)$  and  $y(p)$  are the local coordinates of the intersection point of the ray with the plane given by  $p$ . The slack  $S(p)$  provides a certain measurement of the distance of a point on the ray to the surface of the fibre core. Its value is positive inside the core, and negative for points outside it. Therefore, the following reflection point is at the plane given by the first root of  $S(p) = 0$ .

Each time a ray reaches the core-cladding interface, a generalized Fresnel transmission coefficient  $T$  for curved interfaces [6] can be employed to calculate the fraction of power radiated by the ray into the cladding. The remarkable feature of the power transmission coefficient is that it depends only on the radius of curvature in the plane of incidence and the inclination with respect to the normal to the fibre surface. To a first approach, a possible simplification that yields very similar results [6] is to consider  $T = 1$  for refracting rays and  $T = 0$  otherwise. Our results in this paper correspond to this approach. In addition, the length of the ray path is recorded in order to apply the fibre attenuation coefficient due to material absorption [7]. Eventually, the powers of all the rays reaching the end of the fibre are added to obtain the total output power.

## 3 Results

Our goal has been to simulate the attenuation induced when a typical SI POF is bent forming curves of practical interest, so as to evaluate the influence of the most important geometric parameters in each configuration. Specifically, we have chosen usual values for the core radius (490 $\mu$ m) and for the core and cladding refractive indices (1.492 and

1.402 respectively), yielding a numerical aperture (NA) of 0.5. The emission angle of the light source in our simulations is 40 degrees, corresponding to an NA of 0.34. This is smaller than the POF NA, so no significant losses will appear in a short POF section unless this is bent. The POF attenuation coefficient is 0.16dB/m.

For example, we have found computationally that losses in a helix are very similar to those in a circle provided that the local radius of curvature and the distance covered are the same, although the torsion present in the helix does play some small role in bend losses. For the simulations, we have employed a helix expressed in Cartesian coordinates as  $\{x = a \cos p, y = a \sin p, z = bp\}$  with  $a = r + r_c$ , where  $r$  is the radius of a cylinder around which the fibre is bent,  $r_c$  is its core radius, and  $p$  is the angle rotated around the cylinder. In this case, the local radius of curvature of the fibre axis is given by  $R = (a^2 + b^2) / a$ . In Fig. 1 we have plotted with dashed lines the results obtained for helices in which  $b/a = \tan(45)$ , and with solid lines those corresponding to circle arcs of the same length and bend radius  $R$ , for which  $r$  has been reduced appropriately.

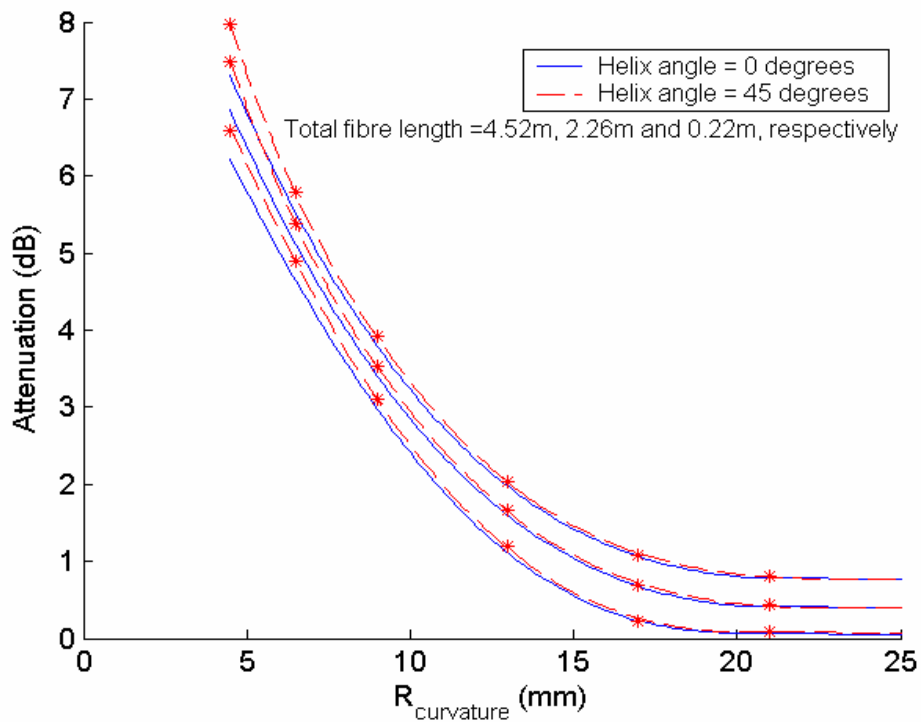


Figure 1. Attenuations for helices with  $b/a = \tan(45)$  (dashed), and for circle arcs of the same length and bend radius  $R$  (solid), for three different fibre lengths.

As could be expected, the results are similar for helical and circular arcs of equal lengths and radii, although the difference is greater when the local radius of curvature is small. For bend radii greater than 20mm, radiation losses are small and in all three cases the attenuation is due almost exclusively to material absorption.

Fig. 2 illustrates the combined effect of two consecutive 90° circular bends of constant radii and arc length, allowing only their relative positions in space to vary. The second bend does not necessarily belong to the same plane as the first one, but to a plane making an angle  $\mathbf{j}$  with it, as shown in Fig. 2 (top).

The reason for choosing this configuration is that, as is well known, two coplanar bends of opposite concavities tend to attenuate considerably more than the same bends with equal concavities. However, if 3-D layouts are considered, there is a continuum of

configurations between these two extreme cases, corresponding to angles  $j = 0$  and  $j = p$  in Fig. 2, so a more detailed study has been carried out. As expected, the attenuation for intermediate values of  $j$  increases monotonously from  $j = 0$  to  $j = p$ . Moreover, the maximum rate of variation occurs in the vicinity of  $j = 90^\circ$ , as marked with a “ $\Delta$ ” in the figure.

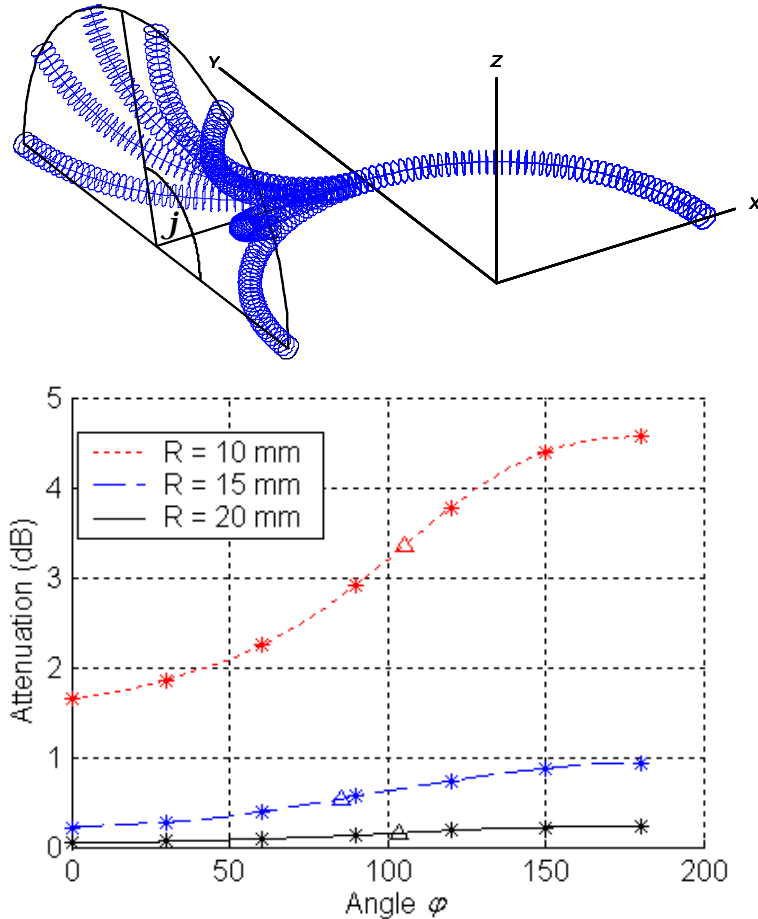


Figure 2. Attenuation in two consecutive  $90^\circ$  circular bends of constant radii and arc length, as a function of the angle  $\varphi$  between their containing planes, for three different bend radii.

In Fig. 3 we show part of a possible layout that could be found in small spaces such as in cars, robots, etc. It should be noted that the three bends are of different radii, which makes the attenuation different depending on the sense in which light propagates. This point has been studied and the results presented in Table 1.

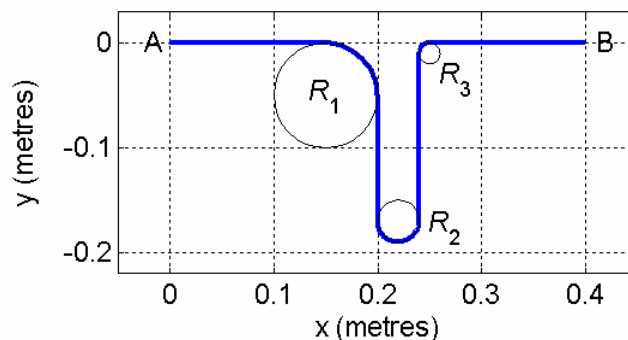


Figure 3. Part of a typical layout in small spaces (cars, robots...) with the POF bent with three different radii, to illustrate the effect of the relative positions of the bends.

It can be seen in Fig. 3 that bend radii of successive bends decrease when propagation takes place in the sense from *A* to *B*, while they increase from *B* to *A*. The broader the input power angular distribution at the entrance of a bend, the greater the radiation loss tends to be, so it is no wonder that, in this case, the total attenuation is higher from *A* to *B* than vice versa. This is because power loss in  $R_3$  is greater than in any other of the bends, irrespectively of the propagation sense, but with a significant difference between the two senses (see Table 1) because  $R_1$  and  $R_2$  have broadened the angular power distribution from *A* towards  $R_3$ .

LIGHT PROPAGATION → ATTENUATION... ↓	From A to B	From B to A
...introduced by $R_1$	0.06dB	0.05dB
...introduced by $R_2$	0.08dB	0.19dB
...introduced by $R_3$	1.68dB	1.42dB
...TOTAL	1.82dB	1.66dB

Table 1. Attenuation produced in the different bends in the layout of Fig. 3, as well as the total attenuation, for both senses of propagation.  $R_1 = 50\text{mm}$ ,  $R_2 = 20\text{mm}$ ,  $R_3 = 10\text{mm}$ .

However, we cannot conclude that attenuation from *A* to *B* is always higher than the opposite for any radius  $R_2$ . On the contrary, when  $R_2$  is sufficiently small, e.g. 10mm, this second curve induces the greatest loss in both senses (see Table 2), determining which sense is better from the point of view of minimum attenuation, which now turns out to be from *A* to *B*. Therefore, it is the curve introducing the greatest losses rather than the last one that tends to determine the influence of interchanging the position of emitter and receiver.

LIGHT PROPAGATION → ATTENUATION... ↓	From A to B	From B to A
...introduced by $R_1$	0.06dB	0.06dB
...introduced by $R_2$	1.90dB	2.44dB
...introduced by $R_3$	1.76dB	1.42dB
...TOTAL	3.72dB	3.92dB

Table 2. Attenuation produced in the different bends in a layout nearly equal to that of Fig. 3, only differing in the radius  $R_2$  of the second cylinder.  $R_1 = 50\text{mm}$ ,  $R_2 = 10\text{mm}$ ,  $R_3 = 10\text{mm}$ .

Finally, a pressure or displacement sensor could be modelled, to a first approach, as a POF in the shape of a sine whose amplitude experiments small variations depending on the displacement of the mould it passes through (Fig. 4, left). We have computationally simulated it for  $n = 4, 5$  and 5 periods respectively, obtaining the results in Fig. 4 (right). It can be seen that there is a region of amplitudes where the slope of the attenuation is near to its maximum, and therefore the sensitivity is optimum. It corresponds to a minimum radius of curvature of the sine of about 10mm, as shown in the upper line of the same figure. It can also be noticed that, as the number of sine periods increases, the sensitivity improves as well.

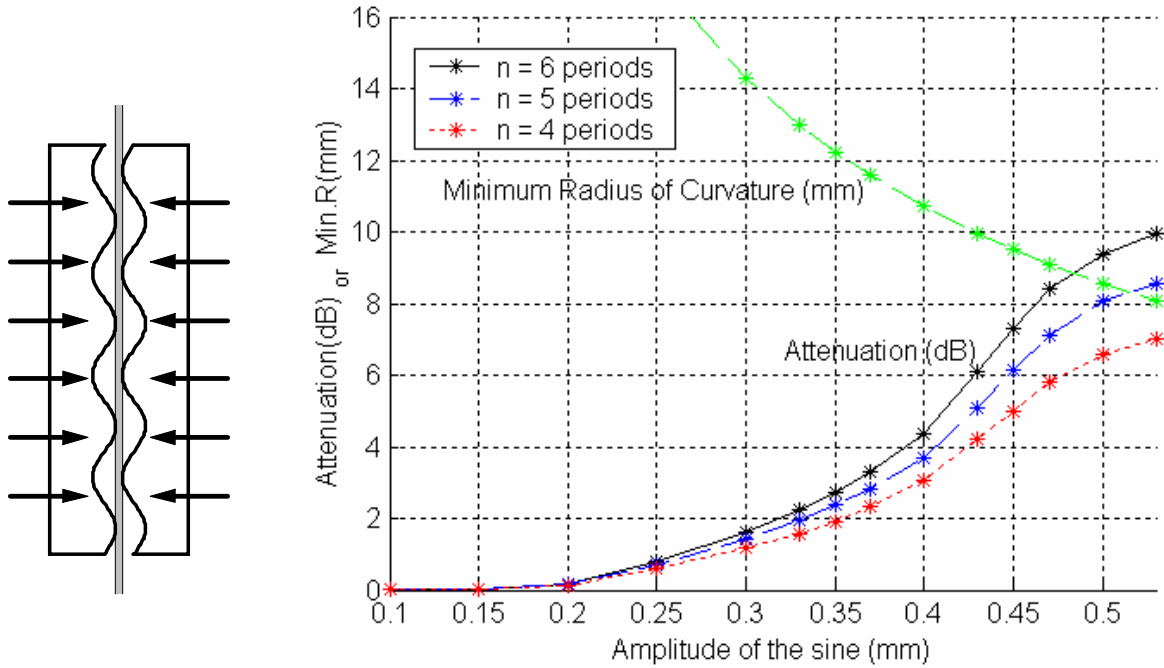


Figure 4. Attenuation against sine amplitude in a simplified displacement sensor.

Another possibility of the program is simulating arbitrary variations in the fibre cross-section geometry: half-axes  $a$  and  $b$ , and the degree of homogeneity  $m$  in Eq. (1). To illustrate the usefulness of this capability we have simulated small periodic perturbations in the amplitude of both half-axes (deviating from the core radius  $r$ ) and in the value of  $m$  (deviating from the circular and elliptical case  $m = 2$ ). These perturbations are schematically shown in Fig. 5.

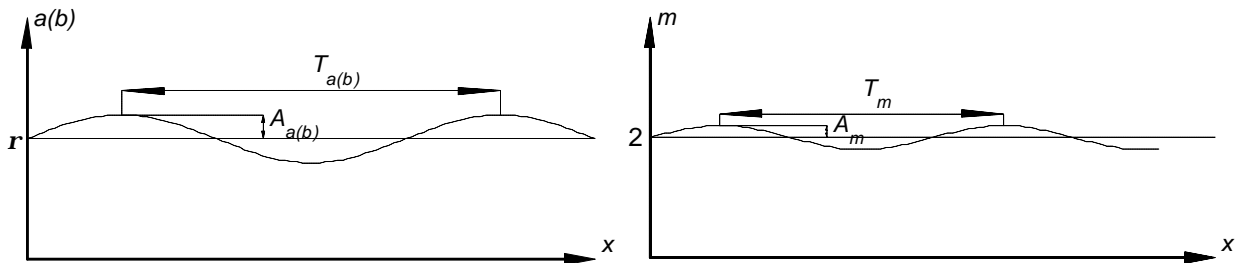


Figure 5. Periodic perturbations in the cross-section parameters  $a$ ,  $b$  and  $m$  of Eq. (1). The variations of  $a$  and  $b$  are independent.

Several simulations with random amplitudes  $A_a$ ,  $A_b$ ,  $A_m$ , and random periods  $T_a$ ,  $T_b$ ,  $T_m$  of the perturbations have been carried out. The main conclusion that can be drawn is that the attenuation is rather sensitive to perturbations in  $m$ . For instance, with constant values  $T_a = 501 \text{ mm}$ ,  $T_b = 782 \text{ mm}$ ,  $T_m = 597 \text{ mm}$ ,  $A_a = 0.31 \text{ mm}$  and  $A_b = 0.09 \text{ mm}$ , if  $A_m = 0$ , the attenuation only changes from 0.026 dB in the unperturbed case to 0.027 dB; however, if  $A_m = 0.008$ , the attenuation increases up to 0.046 dB.

## 5. Conclusions

A new computer program developed by the authors has been used to simulate light propagation in step-index plastic optical fibres of very general 3-D geometry. The results obtained show its usefulness to predict the attenuation of specific links with a given geometry, and to draw rule-of-thumb conclusions that may be valid in a wide variety of

situations, including random perturbations due to imperfections in the fibre cross-section.

### **Acknowledgments**

The authors would like to thank the *Universidad del País Vasco / Euskal Herriko Unibertsitatea* and the *Ministerio de Ciencia y Tecnología* under projects 9/UPV 00147.345-14626/2002ZUBIA, TIC2000-059 and TIC2003-08361 for their financial support.

### **References**

- [1] D. Seidl, P. Merget, J. Schwarz, J. Schneider, R. Weniger and E. Zeeb, Application of POFs in data links of mobile systems, *Proc. Seventh International Conference on Plastic Optical Fibers and Applications POF'98*, 1998, pp.205-211.
- [2] J. Arrue, J. Zubia, G. Fuster and D. Kalymnios, Light power behaviour when bending plastic optical fibres, *IEE Proc.-Optoelectron.*, Vol.145, No.6, 1998, pp.313-318.
- [3] J. Zubia, G. Aldabaldetrekue, G. Durana, J. Arrue, H. Poisel and C. A. Bunge, Geometric optics analysis of multi-step index optical fibers, *Fiber and Integrated Optics*, Vol.23, 2004, pp.121-156.
- [4] J. Zubia and J. Arrue, Plastic Optical Fibers: An Introduction to their Technological Processes and Applications, *Optical Fiber Technology*, Vol.7, 2001, pp.101-140.
- [5] K. F. Barrell and C. Pask, Geometric optics analysis of non-circular, graded-index fibres, *Optical and Quantum Electronics*, Vol.11, 1979, pp.237-251.
- [6] A. W. Snyder and J. D. Love, Reflection at a curved dielectric interface – Electromagnetic Tunneling, *IEEE Trans. Microwave Theory Tech.*, Vol.MTT-23, No.1, 1980, pp.134-141.
- [7] A. W. Snyder and J. Love, *Optical Waveguide Theory*, Chapman & Hall, 1983.